

Spinal Cord Injury Causes Plasticity in a Subpopulation of Lamina I GABAergic Interneurons

Kimberly J. Dougherty and Shawn Hochman

Department of Physiology, Emory University School of Medicine, Atlanta, Georgia

Submitted 4 October 2007; accepted in final form 8 May 2008

Dougherty KJ, Hochman S. Spinal cord injury causes plasticity in a subpopulation of lamina I GABAergic interneurons. *J Neurophysiol* 100: 212–223, 2008. First published May 14, 2008; doi:10.1152/jn.01104.2007. Dysfunction of the spinal GABAergic system has been implicated in pain syndromes following spinal cord injury (SCI). Since lamina I is involved in nociceptive and thermal signaling, we characterized the effects of chronic SCI on the cellular properties of its GABAergic neurons fluorescently identified in spinal slices from GAD67-GFP transgenic mice. Whole cell recordings were obtained from the lumbar cord of 13- to 17-day-old mice, including those having had a thoracic segment (T₈₋₁₁) removed 6–9 days prior to experiments. Following chronic SCI, the distribution, incidence, and firing classes of GFP⁺ cells remained similar to controls, and there were minimal changes in membrane properties in cells that responded to current injection with a single spike. In contrast, cells displaying tonic/initial burst firing had more depolarized membrane potentials, increased steady-state outward currents, and increased spike heights. Moreover, higher firing frequencies and spontaneous plateau potentials were much more prevalent after chronic SCI, and these changes occurred predominantly in cells displaying a tonic firing pattern. Persistent inward currents (PICs) were observed in a similar fraction of cells from spinal transects and may have contributed to these plateaus. Persistent Na⁺ and L-type Ca²⁺ channels likely contributed to the currents as both were identified pharmacologically. In conclusion, chronic SCI induces a plastic response in a subpopulation of lamina I GABAergic interneurons. Alterations are directed toward amplifying neuronal responsiveness. How these changes alter spinal sensory integration and whether they contribute to sensory dysfunction remains to be elucidated.

INTRODUCTION

The most superficial layer of gray matter, lamina I, is a spinal sensory relay site. Nociceptive and thermoreceptive input enters via A δ and C fiber afferents and is transmitted to the thalamus, periaqueductal gray, and parabrachial area via lamina I ascending tract neurons (Craig 2000). GABAergic neurons constitute ~25% of the neuronal population of lamina I (Polgar et al. 2003; Todd and Spike 1993). GABAergic neurons in this region are at a nodal point in the control of pain processing and have been shown to play an important role in spinal cord function and dysfunction, particularly in relation to pain (Coull et al. 2003) and spinal cord injury (Craig 2002; Finnerup and Jensen 2004). Because descending modulatory inputs to the dorsal horn are predominantly inhibitory (Gebhart 2004; Millan 2002), their loss after spinal cord transection likely contributes to hyperexcitability in spinal circuits that can manifest in increased nociceptive reflexes (Suzuki et al. 2004). Resulting hyperexcitability of dorsal horn neurons causes

chronic pain (Malan et al. 2002; Millan 1999; Zeilhofer 2005). GABAergic neurons in lamina I are in a key position for the control of pain transmission. However, the ways in which these cells are affected by chronic spinal cord injury is unknown.

Voltage-gated ion channels, including Na_v1.3, L-type Ca²⁺ (Ca_v1), and T-type Ca²⁺ (Ca_v3) have been linked to spinal hyperexcitability in both injury and pain (Hains et al. 2003a; Heinke et al. 2004a). Most of these same channels have also been implicated in persistent inward currents (PICs) and plateau potentials in both motoneurons and dorsal horn neurons (Hains et al. 2003a; Heckman et al. 2003; Hounsgaard and Kiehn 1989; Morisset and Nagy 1999). Where most studies have been carried out in motoneurons, plateau potentials have been reported in small subpopulations of neurons in the substantia gelatinosa (Yoshimura and Jessell 1989) and deep dorsal horn (Derjean et al. 2003; Monteiro et al. 2006; Morisset and Nagy 1999; Russo and Hounsgaard 1996).

PICs with Na⁺ and/or Ca²⁺ components have been reported in a larger fraction of lamina I (Prescott and De Koninck 2005) and laminae II–IV neurons (Murase et al. 1986). PICs, particularly in the dorsal horn, are modulated by a number of intrinsic spinal and descending supraspinal transmitters including substance P, GABA, glutamate, 5-HT, and acetylcholine (Derjean et al. 2003; Herrero et al. 2000; Murase et al. 1986; Russo et al. 1997, 1998). PICs generating plateaus become more readily activated and more sensitive to modulation in motoneurons in the chronically transected cord (Harvey et al. 2006; Li and Bennett 2003), but the actions of PICs in dorsal horn neurons after chronic cord transection remain unstudied.

Recently, the GAD67-GFP transgenic mouse has proven useful in examinations of spinal GABAergic neurons (Dougherty et al. 2005; Heinke et al. 2004b). We have shown that GAD67-GFP identified lamina I GABAergic neurons divide into at least two different populations of neurons based on their firing properties (Dougherty et al. 2005). Given the importance of GABAergic neurons to the inhibitory control of excess spinal cord excitability after SCI, the main objective of the present study was to determine the effects of complete spinal cord transection on lamina I GABAergic membrane properties, focusing on changes in active cellular properties.

Some results have been presented in abstract form (Dougherty and Hochman 2005, 2006).

METHODS

All experimental procedures complied with the National Institutes of Health guidelines for animal care and the Emory Institutional

Address for reprint requests and other correspondence: S. Hochman, Whitehead Biomedical Research Bldg., Rm. 644, Emory University School of Medicine, 615 Michael St., Atlanta GA 30322 (E-mail: shochm2@emory.edu).

The costs of publication of this article were defrayed in part by the payment of page charges. The article must therefore be hereby marked "advertisement" in accordance with 18 U.S.C. Section 1734 solely to indicate this fact.

Animal Care and Use Committee. Homozygotic GAD67-GFP mice obtained from Jackson Laboratory (Bar Harbor, ME) were used in all experiments. Lamina I was identified between the dorsal white matter and the relatively translucent substantia gelatinosa. No cell $>20\ \mu\text{m}$ from the edge of the white matter was considered (Chery et al. 2000). Some lamina I neurons may have been excluded from consideration because lamina I is thicker in the central part of the cord.

Spinal cord transection

Mice, postnatal day (P) 6–8, were anesthetized with 10% urethane (1.5 mg/kg). Following dorsal laminectomy to expose a segment of the thoracic spinal cord, one segment between T₈ and T₁₁ was removed. Gel foam was used to maintain the separation between rostral and caudal parts of the cord. Mice recovered for 6–9 days (mean = 8) before cell counting or electrophysiology experiments at P13–17 (mean = 15).

Surface area and cell counts

Mice at postnatal day (P) 14 were anesthetized with urethane (2 mg/kg ip) and perfused with 1:3 volume/body weight ice-cold 0.9% NaCl-0.1% NaNO₂, 1 unit/ml heparin, followed by equal volume/body weight of 4% paraformaldehyde or modified Lana's fixative (4% paraformaldehyde, 0.2% picric acid, 0.16 M PO₃); pH 6.9. All spinal cords were isolated and postfixed 1 h, cryoprotected in 10% sucrose, 0.1 M PO₃, pH 7.4 until sectioned in 10- μm -thick slices on a cryostat (Leitz 1720).

Ten nonconsecutive sections (100 μm apart) from lumbar segments 1–3 of three control mice and three chronic SCI mice were used for comparison of surface area and lamina I cell numbers using the NeuroLucida image analysis system (MicroBrightField, Williston, VT). All cell counts can only be regarded as estimates since stereological techniques were not used. This should not affect comparisons between treatment groups.

Electrophysiology

Control and chronic SCI mice (P13–17) were anesthetized with urethane (2 mg/kg ip) and decapitated, and the spinal cord was carefully dissected out of the body cavity and placed in a cooled ($<4^{\circ}\text{C}$) artificial cerebrospinal fluid (ACSF) containing (in mM) 250 sucrose, 2.5 KCl, 2 CaCl₂, 1 MgCl₂, 25 glucose, 1.25 NaH₂PO₄, and 26 NaHCO₃ at a pH of 7.4. The ACSF was continuously oxygenated with 95% O₂-5% CO₂. Transverse (150–250 μm) spinal slices were cut from lumbar cord using a vibrating blade microtome (Leica VT1000 S). Slices were left to recover at room temperature for ≥ 1 h prior to the onset of experimentation. The slicing procedure was common to both groups and represents an acute spinal injury. Because an acute injury is implicit to these procedures, for simplicity we refer to the acutely injured group as the controls and to the mice with a chronic spinal transection followed by the acute injury as the SCI or spinal cord transected mice.

Patch electrodes were prepared from 1.5 mm OD capillary tubes (World Precision Instruments, Sarasota, FL) using a two-stage puller (Narishige PP83) to produce resistance values ranging from 5 to 8 M Ω . For the majority of the experiments, the intracellular recording solution contained (in mM) 140 K-gluconate or KF, 11 EGTA, 10 HEPES, 1 CaCl₂, and 35 KOH, pH 7.3. In some electrodes, a support solution of 4 mM ATP and 1 mM GTP was also included. No differences in properties were observed between electrodes containing or not containing support solution. For some voltage-clamp experiments, intracellular recording solution contained (in mM) 120 CsF, 10 EGTA, 10 HEPES, 10 CsCl₂, and 35 CsOH.

The recording chamber was continuously perfused with oxygenated ACSF (in mM: 125 NaCl, 2.5 KCl, 2 CaCl₂, 1 MgCl₂, 25 glucose, 1.25 NaH₂PO₄, and 26 NaHCO₃ at a pH of 7.4) at a rate of ~ 2

ml/min. In some voltage-clamp experiments, the K⁺ channel blockers 4-aminopyridine (4-AP; 2 mM) and tetraethylammonium (TEA; 10 mM) were included in the perfusion ACSF (as noted in RESULTS).

Whole cell patch-clamp recordings were undertaken at room temperature using the Multiclamp amplifier (Axon Instruments; Union City, CA) filtered at 5 kHz (4-pole low-pass Bessel). GFP⁺ lamina I interneurons were identified using epifluorescent illumination. Position of the cell in lamina I was verified using differential-interference contrast optics (DIC) at $\times 40$ to show that the cell was in or adjacent to the white matter in that focal plane (Chen and Gu 2005). Then the electrode was lowered into the slice and the cell targeted for whole cell patch-clamp recordings using DIC. Both voltage- and current-clamp data were acquired on computer with the pCLAMP acquisition software Clampex (v 9.2; Molecular Devices; Union City, CA).

Immediately following rupture of the cell membrane (in voltage clamp at -80 mV), the current-clamp recording configuration was used to determine resting membrane potential (except when CsF electrodes used). Series resistance was subtracted. Experiments were conducted in both current- and voltage-clamp modes. In current clamp, cells were brought to -80 mV by injecting bias current through the headstage. Then a series of 1-s hyperpolarizing and depolarizing current steps were undertaken. Liquid junction potentials were not corrected for. Firing type was determined by the response to current steps at and above threshold (Prescott and De Koninck 2002; Ruscheweyh and Sandkuhler 2002). Membrane properties were measured and calculated as previously described (Dougherty et al. 2005). Peak inward currents were the maximum negative values measured during the first 20 ms of 100-ms voltage steps (-130 to $+70$ mV) from a holding potential of -80 mV. Outward currents were measured as the average current during the last 20 ms of the highest voltage step in the same protocol. Voltage ramps (100 mV, 10 or 20 mV/s) starting at -110 mV were used to examine PICs.

In some experiments, channel blockers were applied using a local perfusion system (SF-77B Perfusion Fast-Step; Warner Instrument, Hamden, CT). The following channel blockers were used (all from Sigma unless stated otherwise): tetrodotoxin (TTX; voltage-gated Na⁺; 1 μM), riluzole (persistent Na⁺; 10 μM ; Tocris), CdCl₂ (non-specific Ca²⁺; 400 μM), NiCl₂ (T-type Ca²⁺; 100 μM), verapamil (L-type Ca²⁺; 50 μM), nifedipine (L-type Ca²⁺; 50 μM). Leak subtraction was performed on all current responses to voltage ramps using Clampfit (Kuo et al. 2005). Resistance was measured from the initial portion of the response where the slope was constant (1st 1.0–1.3 s).

A total of 162 lamina I GFP⁺ cells from 57 control mice and 90 cells from 23 SCI mice with resting potentials more negative than -40 mV were included in the analysis. However, for comparison of cell membrane properties other than resting potentials, only cells with a membrane potential more negative than -50 mV were considered. Statistical comparisons between firing properties were made using a Student's *t*-test and reported as means \pm SE. When distributions were not normal, a Mann-Whitney test was used. When distributions had unequal SDs, a Welch correction was used (InStat, GraphPad Software, San Diego, CA).

RESULTS

Behavior and white/gray matter appearance

Comparisons of thoracic spinal cord transections performed in neonate, weanling, and adult rodents have been previously described in great detail (Stelzner et al. 1975, 1979). Consistent with these reports, we observed hyperreflexive responses to develop in all mice within the first 5 postoperative days and weight support in some mice 7–8 days after spinal cord transection. Some mice did show stepping motions with their hindlimbs, particularly when moving over cage bedding (Guer-

tin 2005; Stelzner et al. 1979). There were no obvious correlations between behavior at the time of the experiment and results from cell recordings.

By 1 wk following spinal cord transection, white matter tracts were noticeably reduced (Fig. 1, *A* and *B*). Overall there was not a significant change in the surface area of the gray matter following spinal transection. However, measured ratios of white matter area to whole cord area demonstrated that white matter tracts had significantly degenerated in the SCI mice and constituted a smaller proportion of the cord area ($32 \pm 2\%$) after the week post injury as compared with the controls ($42 \pm 2\%$; $P < 0.05$) (cf. Anelli et al. 2007).

Counts of GFP⁺ cells in lamina I demonstrated no difference in the number of GABAergic neurons between control (mean = 13 ± 1 per 10- μm section) and SCI mice (mean = 11 ± 2 per 10- μm section).

Incidence of firing properties

In cells from both control and SCI mice, three firing properties were seen in GFP⁺ lamina I neurons – tonic, initial burst, and single spike (Dougherty et al. 2005). The incidence of

firing properties encountered were not statistically different between cells from control and spinal transected mice ($P = 0.45$ Fisher's exact test). Tonic firing cells made up 34% of the control population and 42% of the population from SCI mice. Initial burst cells were encountered in 28 and 27% of cells from control and SCI mice, respectively. Thirty-four percent of control cells and 26% of cells from SCI mice were single spike. The remaining cells were unclassified (4% control, 6% SCI).

Cellular properties

Resting membrane potentials were compared between the control and SCI population (Fig. 2). When binned in 5-mV intervals and plotted as percent incidence, cells from both control and spinal transected mice show apparent bimodal distributions. The more depolarized peak is at -40 mV in both. However, the more hyperpolarized peak is 5 mV more hyperpolarized in cells from controls than in cells from SCI mice, suggesting that a subpopulation of neurons have undergone a depolarizing shift in their resting membrane potential. Shifting the control peak by 5 mV toward 0 aligns the distributions (Fig. 2, dashed line).

There were no differences in resistance, membrane time constant, cell capacitance, rheobase, and voltage threshold between the control and SCI cell populations. However, significant changes in membrane potential, steady-state outward currents and spike heights were observed (Table 1). Membrane potentials were more depolarized in cells from SCI mice (-59 mV) as compared with controls (-63 mV). Cells from SCI mice also had larger spikes (59 vs. 53 mV) and steady-state outward currents (1,170 vs. 1,475 pA).

Correlations between various membrane properties were compared (see Dougherty et al. 2005). For any two measured membrane properties, there were no overall differences in regression coefficients between cells from control and SCI mice or any evidence of changed distributions in neuron subpopulations based on firing type (data not shown). For example, in cells from control and SCI mice there was the same positive correlation between input resistance and membrane time constant ($r = 0.56$ in control and $r = 0.59$ in SCI mice), negative correlation between rheobase and membrane time constant ($r = -0.72$ and $r = -0.70$, in control and SCI mice, respectively), and lack of correlation between resistance and membrane potential ($r = 0.15$ in control, $r = 0.11$ in SCI mice).

Spinal transection-induced changes based on firing type

Single spike cells were unchanged in all properties measured in the cells from SCI mice except action potential decay slope (Fig. 3). We previously reported that the measured membrane properties of tonic and initial burst cells were indistinguishable in controls (Dougherty et al. 2005). When grouping these neuron populations, membrane potential, steady-state outward current, spike height, and action potential decay slope were all altered in cells from SCI mice. Unlike controls, the membrane properties of tonic and initial burst firing types differed within the cell population from SCI mice. Rheobase was lower (49 vs. 74 pA; $P < 0.01$) and maximum firing frequency was higher (54 vs. 32 Hz; $P < 0.0001$) in cells firing tonically. Moreover, the tonically firing

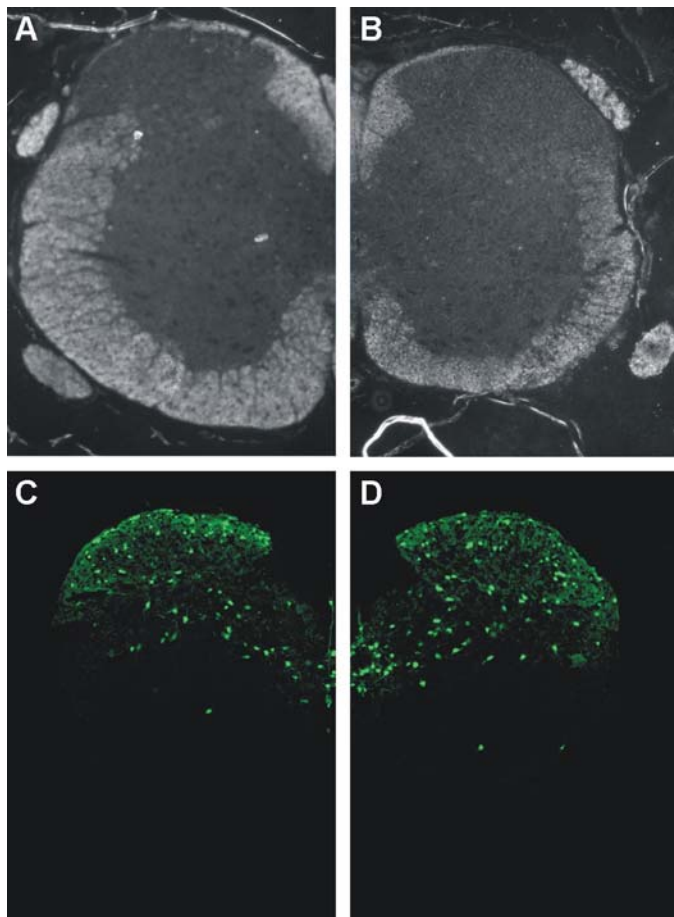


FIG. 1. Spinal cord of GAD67-GFP mouse 1 wk after spinal transection. Transverse spinal slices (10 μm) taken from lumbar cord of P14 control (*A* and *C*) and spinal transected (*B* and *D*) mice. The area occupied by the white matter tracts is reduced in the slice from the spinal cord injured (SCI) mouse (*B*) as compared with the control (*A*). Overall GFP⁺ distribution appears the same between control (*C*) and SCI (*D*) mice.

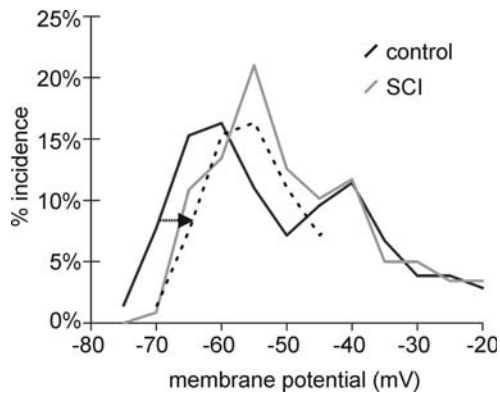


FIG. 2. Resting membrane potential distribution of cells from control (black) and SCI (gray) mice. Both cell types show an apparent bimodal distribution. The first peak of cells from controls is more hyperpolarized than that of cells from SCI mice. A 5-mV shift of the first control peak (dashed black) lines up well with the 1st SCI peak.

cells from SCI mice also had a higher maximum firing frequency than the control tonic cells (43 Hz; $P < 0.05$).

Firing frequency

A subset of cells from spinal transected mice had noticeably higher firing rates than control cells (Fig. 4, *A* and *B*). Additionally, in two cells from SCI mice, plateau potentials were evident around rheobase (Fig. 4*C*). These plateaus were never seen during current step protocols in controls.

Instantaneous firing frequencies of tonic and initial burst cells were compared in cells from both control and SCI mice and plotted against injected current (the *f-I* curve; Fig. 5). When firing was divided into three firing ranges, most cells from both control and spinal transected mice had low firing frequencies (Fig. 5, *A* and *B*, dark gray shaded region). Despite the smaller number of cells from SCI mice displayed, it is clear that more neurons from spinal transected mice fired with high and moderate frequencies. One cell from a SCI mouse fired with a very high frequency. Regression lines show that, overall, cells from SCI mice fire with higher firing frequencies in response to current injections between ~ 30 and ~ 115 pA (Fig. 5*C*). Interestingly, separation of neurons according to tonic and initial burst firing shows that it is the tonic cells that fired with higher frequencies following spinal transection (Fig. 5*D*; black and white lines, respectively, in Fig. 5, *A* and *B*).

Spontaneous plateau potentials

Evidence of spontaneous plateau potentials was seen in few cells from control mice (7%). However, 27% of cells from SCI mice displayed at least one spontaneous plateau potential during continuous recordings. Plateaus were most commonly seen in tonically firing cells. Their duration ranged from short (~ 50 ms) to very long duration (~ 50 s) although most ($\sim 75\%$) were ≤ 1 s in duration. Plateaus spontaneously occurred within a membrane potential range of -120 to -40 mV with values ranging from -80 to -15 mV. In a recording from a particularly active cell from a spinal transected mouse (Fig. 6), the heterogeneity of plateau duration and magnitude is obvious. The increased incidence of spontaneous plateaus suggests there

may be an increase in the expression of PICs, which would also contribute to the higher firing frequencies seen with *f-I* curves (Kuo et al. 2006).

Persistent inward currents in control cells

PICs were examined using triangular voltage ramps (-110 to -10 mV) over 5 or 10 s. PICs were not evident in most neurons in control mice (-11 ± 4 pA; Fig. 7*A*). However, following blockade of voltage-gated K^+ channels with intracellular Cs and extracellular 4-AP and TEA, PICs were seen in all cells tested ($n = 27$, Fig. 7*B*). For the rising phase, PIC amplitudes were -38 ± 5 pA in 5-s ramps and approximately double in 10-s ramps (-75 ± 20 pA), and the corresponding falling phase values were -48 ± 6 and -104 ± 22 pA in 5- and 10-s ramps, respectively. The membrane potentials at the peak amplitudes during rise (-40 ± 2 mV) and falling phases (-46 ± 3 mV) were comparable.

TTX blocked the majority of the PIC with peak current of the rising and falling phases reduced to 12 and 38% of the control (Fig. 7*D*). In comparison, riluzole, the persistent sodium channel blocker (Fig. 7*E*) reduced the peak amplitude of the rising phase to 60% of control. The descending phase was also reduced, to 70% of the peak amplitude of control (Fig. 7*C*).

The Ca^{2+} channel blocker Cd^{2+} blocked most of the rising phase of the ramp current (96%) and partially blocked the falling phase (left 39% of the control remaining; $n = 2$). Ni^{2+} , a T-type Ca^{2+} channel blocker ($n = 2$), had no effect on either rising or falling phase PIC amplitude. The L-type Ca^{2+} channel blockers, nifedipine and verapamil, reduced both rising and falling phases of the voltage ramps. Nifedipine ($n = 7$) reduced the PIC to 49% of control values on rising and 68% on the falling phase (Fig. 7). Verapamil had weaker actions. In two of three cells tested, verapamil reduced PIC amplitude to 87 and 77% of control rising and falling phase values, respectively. In summary, both voltage-gated Na^+ and Ca^{2+} currents contribute to PICs.

While pharmacological characterization of the conductances underlying PICs in neurons in SCI mice was not performed, under normal recording conditions, the responses to voltage ramps were not significantly different from controls ($n = 32$; Fig. 8*A1*). However, in 28% of these cells, a high-threshold inward current is activated and can be seen in the falling

TABLE 1. Comparison of intrinsic membrane properties between cells from control and SCI mice

	Control ($n = 120$)	SCI ($n = 65$)
Resting membrane potential, mV	-63 ± 1	$-59 \pm 1^{***}$
Resistance, M Ω	513 ± 26	557 ± 44
Time constant, ms	23 ± 4	22 ± 2
Capacitance, pF	51 ± 3	47 ± 4
Steady-state outward current, pA	1170 ± 69	$1475 \pm 93^{**}$
Peak inward current, pA	-1584 ± 87	-1673 ± 108
Rheobase, mV	91 ± 6	86 ± 9
Spike height, mV	53 ± 2	$59 \pm 2^*$
Overshoot, mV	16 ± 1	16 ± 1
Voltage threshold, mV	-45 ± 1	-47 ± 1

For comparison of cellular properties, cells with membrane potentials more negative than -50 were considered. SCI, spinal cord injury. $^*P < 0.05$, $^{**}P < 0.01$, $^{***}P < 0.0001$.

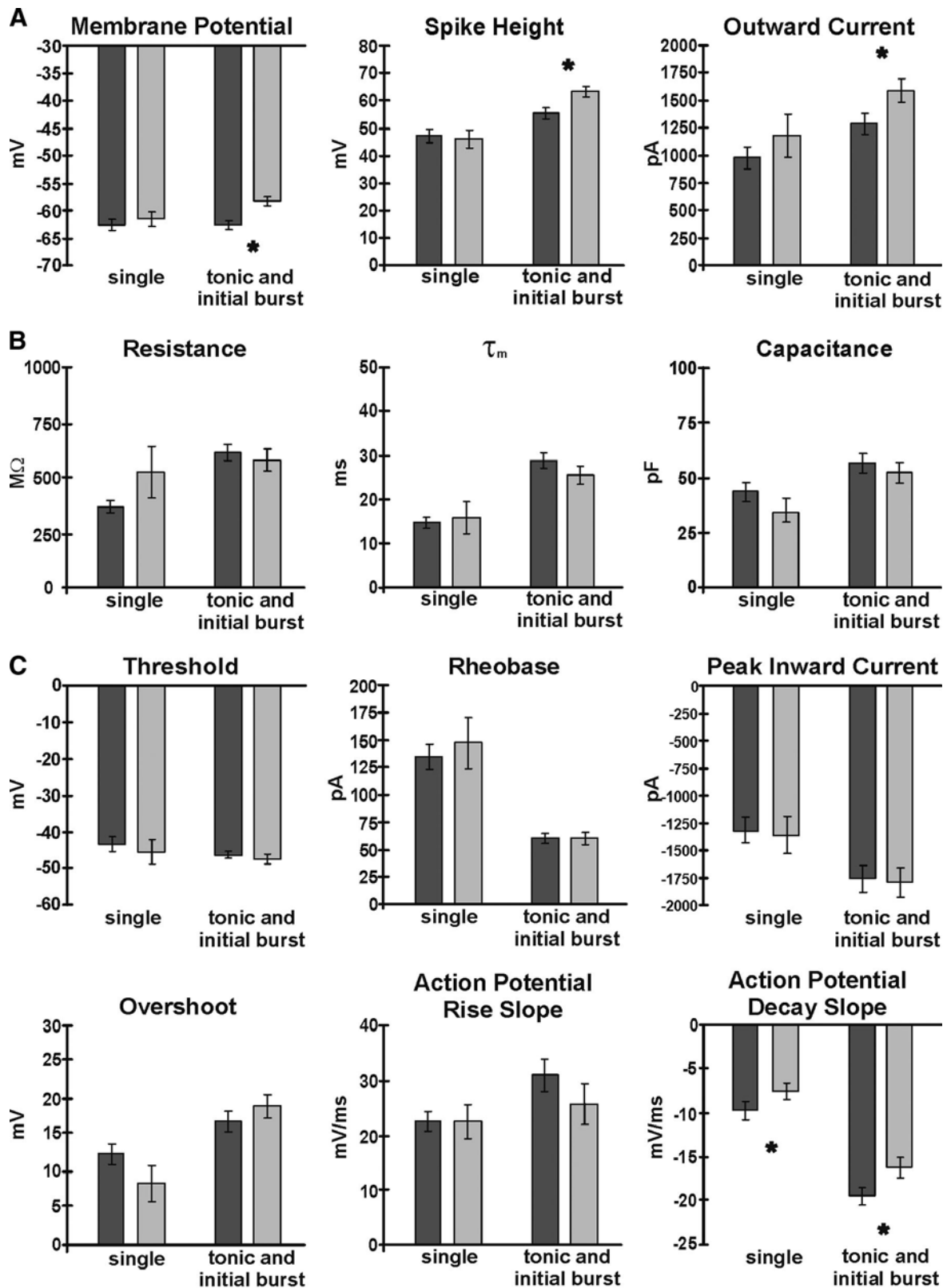


FIG. 3. Comparison of passive and active membrane properties in cells from control and SCI mice divided into 2 separable groups based on firing properties. ■, control means; □, SCI means. Data are presented as means \pm SE. *, statistical significance ($P < 0.05$). *A*: following spinal transection, tonic/initial burst cells had more depolarized membrane potentials, larger steady-state outward currents, and larger spike heights. *B*: the other passive properties measured (resistance, τ_m , and cell capacitance) remained unchanged. *C*: voltage threshold, rheobase, peak inward current, and overshoot were statistically unchanged. While the rise slope was unchanged, the decay slope was less steep in cells from spinal transects.

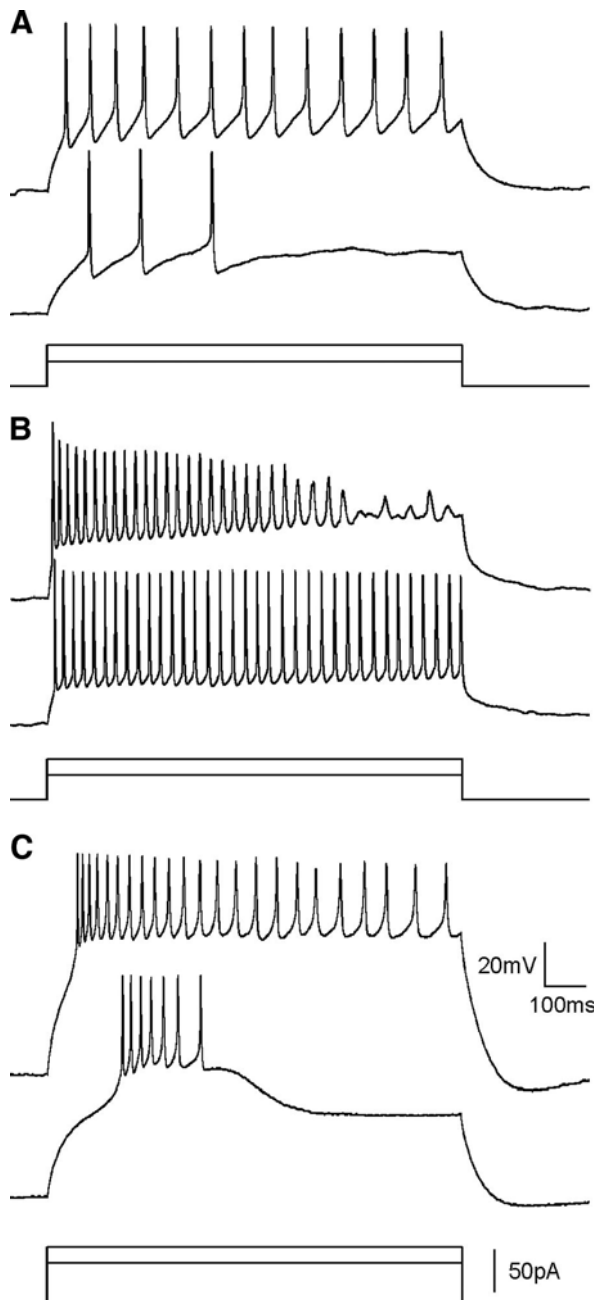


FIG. 4. Tonic cells fire faster in SCI mice. Firing properties displayed were produced by current steps of differing magnitudes as shown in the bottom of each panel. *A*: example of a tonic cell from a control mouse. *B*: example of a faster firing tonic cell from a spinal transected mouse. *C*: Ca^{2+} plateaus with spiking were seen in 2 cells following spinal transection. Scale bars in *C* also correspond to *A* and *B*.

(repolarizing) phase of the voltage-clamp ramp (Fig. 8A2). In these cells, the falling phase of the ramps had larger peak amplitudes than controls (-30 vs. -11 pA; $P < 0.05$). In long voltage step protocols (5 s), a high-threshold current with delayed activation and no inactivation was seen (Fig. 8B). These currents activated at approximately -30 mV, and maximum current varied but was usually 100–250 pA. None of these cells showed either accelerated firing during current steps, a sustained depolarization beyond current steps (Fig. 8C), or enhanced firing on the repolarizing side of a current ramp (Fig. 8D).

DISCUSSION

We sought to determine the effects of SCI on lamina I GABAergic neurons using a complete transection model of SCI. A subset of GABAergic neurons became more excitable following injury as seen by depolarized membrane potentials, larger spike heights, increases in firing frequencies, and increased incidence of spontaneous plateau potentials. In looking for the ionic basis for the plateau potentials, we found that all lamina I GABAergic neurons have PICs mediated by persistent Na^+ and/or L-type Ca^{2+} channels. However, these channels are likely on distal dendrites because they emerged only after facilitating space clamp voltage control with the addition of K^+ channel blockers. Notably, following spinal cord transection, a high-threshold, non-inactivating PIC emerges in approximately the same incidence of neurons at which spontaneous plateaus were encountered.

Effects of injury on the spinal GABAergic system

Approximately 2/3 of SCI patients suffer from chronic pain (Finnerup and Jensen 2004), and numerous studies have demonstrated a hyper-responsive sensory apparatus after SCI (Bennett et al. 1999; Drew et al. 2001; Hains et al. 2003b; Hao et al. 2004; Zhang et al. 2005). GABAergic control of spinal excitability becomes critical after the loss of descending inhibitory controls (Millan 2002), and dysfunction in spinal inhibitory systems has been implicated in altered nociceptive activity (Baba et al. 2003; Coull et al. 2003; Drew et al. 2004; Hao et al. 1992; Moore et al. 2002; Stiller et al. 1996). Caudal to chronic cord transection, GAD-67 expression increases (Tillakaratne et al. 2000) as does afferent-evoked GABAergic synaptic actions (Garraway and Mendell 2007). These processes are likely highly dynamic as increased GAD67 expression can be normalized by exercise training (Tillakaratne et al. 2002). Here, in lamina I, there was no difference in the number, apparent distribution, or incidence of functional subpopulations of EGFP⁺ neurons ~8 days postspinalization.

Excitability increases in a subset of GABAergic neurons following spinal transection

Interestingly, changes in cellular properties following spinalization were largely restricted to a cell subpopulation of lamina I GABAergic interneurons, those that respond to depolarizing currents steps with tonic and initial burst firing. The observed changes all appear to function to increase cell excitability. In comparison, no changes were seen in membrane properties of lamina II GABAergic neurons following chronic constriction nerve injury (Schoffnegger et al. 2006). One of the more striking observations was a depolarizing shift in the membrane potentials of cells from SCI mice. It is possible that an injury-related change in the Cl^- gradient (Coull et al. 2003) may contribute to this. Because voltage threshold and rheobase were unchanged, synaptic and excitatory neuromodulatory events would be much more likely to recruit these neurons. Additionally, observed increases in spike height and outward current could contribute to an increase in excitability. An increase in spike height may be due to changes in voltage-gated Na^+ or K^+ channels (Chen et al. 1996; Kang et al. 2000; Melnick et al. 2004). The increase in spike heights is likely due to a decrease or

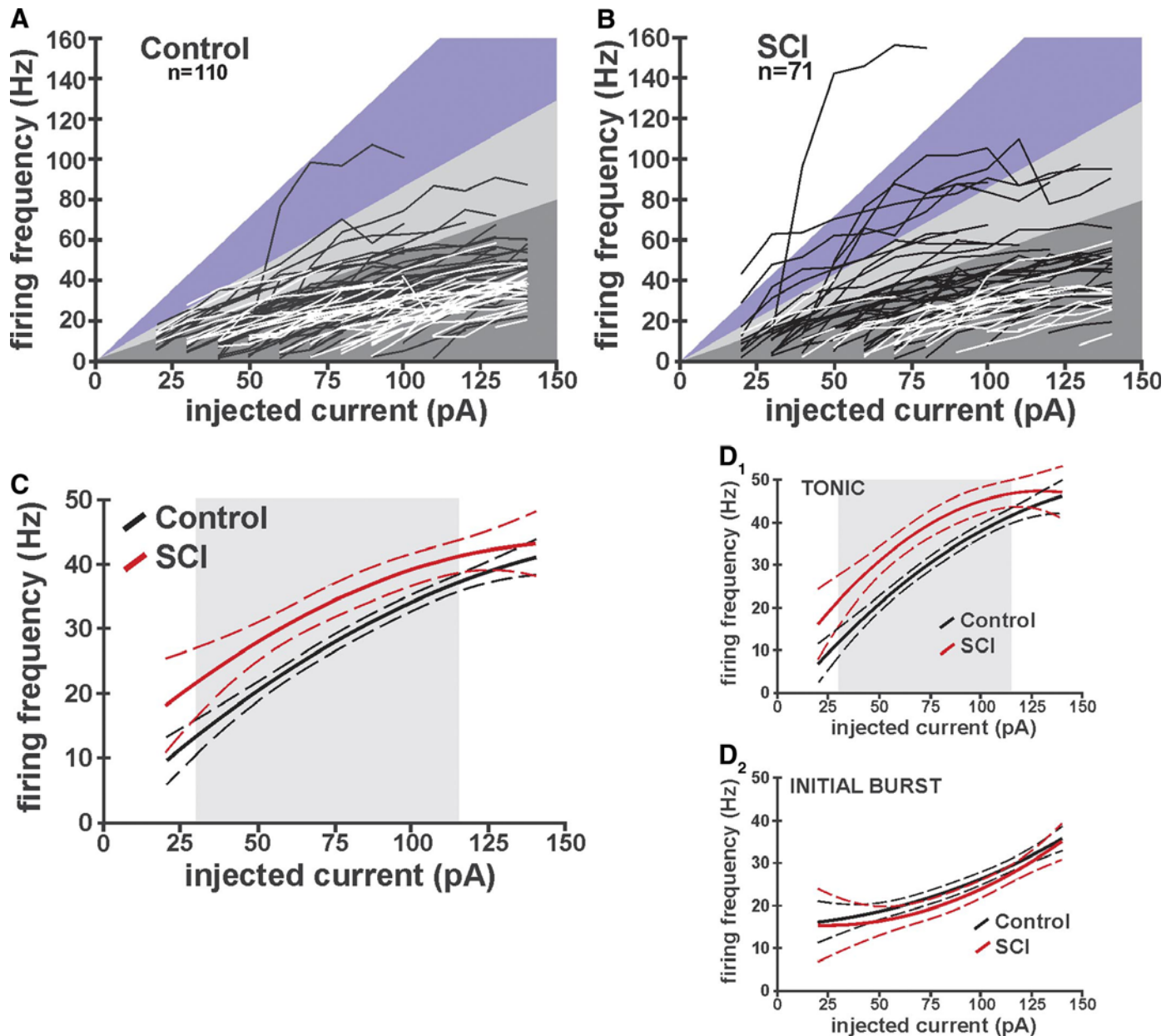


FIG. 5. Frequency-current ($f-I$) relationships for cells from control and SCI mice. Firing frequency was measured as the interspike interval between the 1st 2 spikes in response to current injection. Many of the cells from SCI mice (*B*) had firing frequencies in the same range as controls (*A*; dark and light gray shaded region). However, a subpopulation of cells fired with faster frequencies (purple and white). Shading in *A* and *B* was chosen to highlight differences. Black lines represent tonic cells and white lines represent initial burst cells. Note that, with few exceptions, all initial burst cells from both control and SCI mice are in the dark gray region. *C*: polynomial best fit of control and spinal transect $f-I$ curves shows that cells from SCI mice have higher firing frequencies over the midrange of injected current (30–115 pA; gray box). Dashed lines represent 95% confidence intervals. *D*: polynomial best fit of control and SCI $f-I$ curves do not overlap in tonic cells (*D1*) but do in initial burst cells (*D2*).

change in K^+ channel properties. Because the rising slope of the spike and peak inward currents remained unchanged while action potential decay was faster, K^+ channels responsible for fast repolarization (A-current) are implicated (Chen et al. 1996; Kang et al. 2000). Alternatively, this could be due to changes in the kinetics of Na^+ channels or a shift in the voltage dependence due to changes in auxiliary subunits (McCormick et al. 1999; Meadows et al. 2002). The increase in peak steady-state outward currents following spinal transection suggests that one of the delayed rectifier K^+ channels is facilitated and is consistent with faster firing frequencies (Melnick et al. 2004). Also even

though the changes were not significant, voltage thresholds of cells from SCI mice tended to be more hyperpolarized.

Spinal cord transection causes firing frequencies of tonic cells to increase

This is the first study to examine the effects of cord transection on lamina I GABAergic neurons, and we show evidence of an increased firing frequency in a subset of tonic cells. Increased spinal excitability and increases in cell firing rates have been reported following cord injury (Hains et al. 2003a; Millan 2002) and in pain models (Finnerup and Jensen 2004;

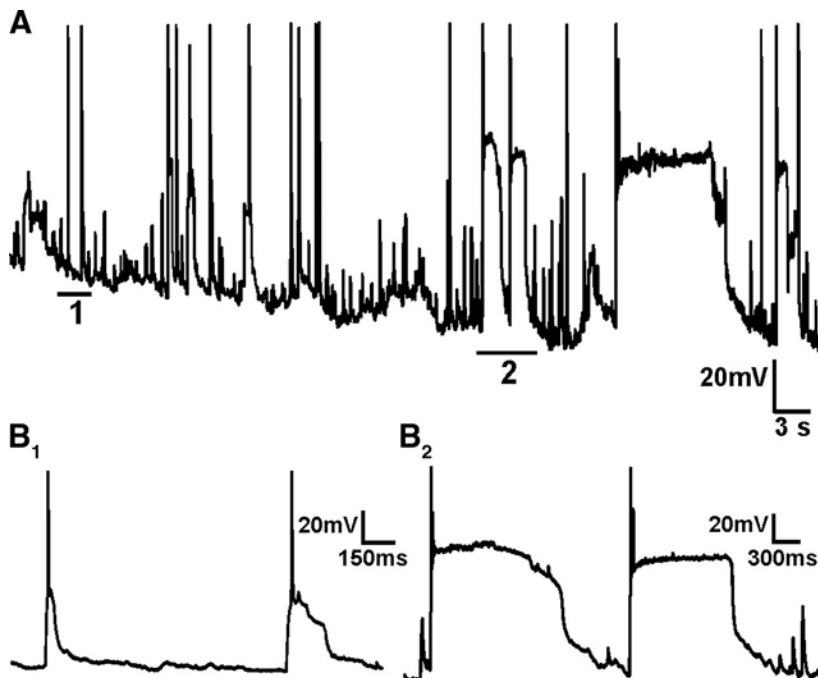


FIG. 6. Spontaneous plateau potentials in cells from SCI mice. *A*: continuous current-clamp recording beginning at -60 mV from a cell with spontaneous plateau potentials. Numbered bars indicate areas expanded in *B*. Demonstrating the range in plateau potentials, 2 examples are shown: short-duration plateaus with small depolarizations (*B1*) and long duration, more depolarized plateaus (*B2*).

Pitcher and Henry 2000), and a loss of inhibitory function has been implicated in pain following injury (Burchiel and Hsu 2001; Wiesenfeld-Hallin et al. 1997) and pain in general (Malan et al. 2002; Millan 1999; Zeilhofer 2005). While there have been no studies directly examining changes in the excitability of inhibitory neurons, based on the aforementioned studies, one would predict reduced excitability. On the other hand, following the loss of descending inhibition, compensatory homeostatic mechanisms intrinsic to the spinal cord may warrant the increases as seen here, in GAD-67 expression (Tillakaratne et al. 2000) and in afferent-evoked GABAergic synaptic actions (Garraway and Mendell 2007).

Increases in firing frequency were specific to tonic firing cells, presumably to result in stronger inhibitory actions on spinal circuits. Because only 11% of lamina I cells are local interneurons (Bice and Beal 1997), and GABAergic neurons comprise 1/4 of the lamina I population (Polgar et al. 2003; Todd and Spike 1993), some GABAergic cells must be propriospinal neurons. Most tonic and initial burst cells are the larger fusiform cells rather than small multipolar, single spike cells (Dougherty et al. 2005). Therefore tonic cells may be propriospinal neurons with more widespread projections. Hence their lesion-induced excitability increase may exert more widespread compensatory inhibitory actions. In contrast, single spike cells may be local circuit interneurons and less relevant to the control of and compensatory response to overall spinal hyperexcitability.

Spontaneous plateaus are more frequent and PICs are evident in cells from SCI mice

As seen in unidentified neurons in the substantia gelatinosa (Yoshimura and Jessell 1989) and deep dorsal horn (Derjean et al. 2003; Monteiro et al. 2006), only a small proportion of lamina I GABAergic neurons have spontaneous plateau poten-

tials. However, a greater number of cells displayed plateaus following chronic cord injury. Plateau potentials depend on neuromodulation in motoneurons (Hounsgaard and Kiehn 1985). Interestingly, plateau potentials disappear after acute cord transection but re-emerge much more prominently in chronically spinal transected rodents (Li and Bennett 2003) and appear to be one mechanism that results in hyperreflexia and spasticity (Bennett et al. 2004).

PICs underlie the plateaus in motor (Carlin et al. 2000; Heckman et al. 2003; Hounsgaard and Kiehn 1989; Li and Bennett 2003), deep dorsal horn (Morisset and Nagy 1999), and ventral horn neurons (Theiss et al. 2007). In particular, L-type Ca^{2+} currents and persistent Na^{+} currents are responsible, both in normal (Hounsgaard and Kiehn 1989; Kuo et al. 2005) and in chronically transected (Li and Bennett 2003) animals. Both persistent Na^{+} and persistent Ca^{2+} currents have been demonstrated in lamina I tonically firing cells where they amplify and prolong depolarization (Prescott and De Koninck 2005).

PICs were not found in normal recording conditions in most cells from control or SCI mice. Following K^{+} current blockade with Cs^{+} (and in some cases 4-AP and TEA), persistent currents were seen in all cells tested. Although firing properties could not be measured in these cells, it is likely that PICs are present in all GABAergic cells in lamina I, regardless of firing type. This conflicts with reports that only tonic cells in lamina I have PICs (Prescott and De Koninck 2005). It is possible that differences in the protocols used to evoke the PICs, differences in the recording conditions, or bias toward excitatory cell types may be responsible for the conflicting results. Because the currents were evident only after K^{+} channel blockade, it is likely that the channels underlying these currents are on the distal dendrites (Carlin et al. 2000; Hounsgaard and Kiehn 1993; Russo and Hounsgaard 1996). Both persistent Na^{+} channel blockers and L-type Ca^{2+} channel blockers were effective at reducing the currents. A model of PICs in tonic

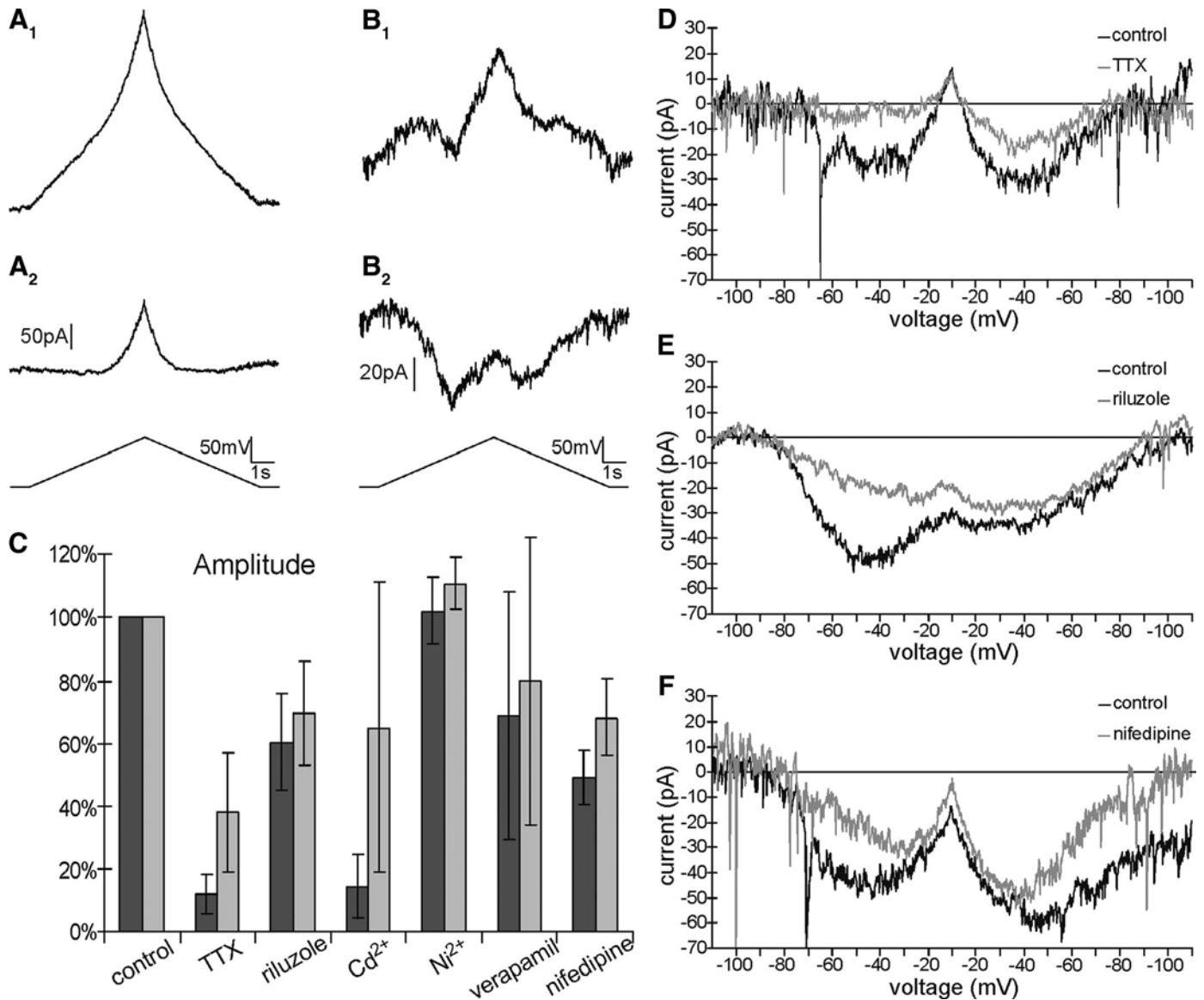


FIG. 7. Persistent inward currents (PICs) in control cells emerge following K^+ channel blockade and are partially blocked by both Na^+ channel and Ca^{2+} channel blockers. *A1*: example of a response to a voltage-clamp ramp in normal recording conditions. *A2*: resulting currents after leak subtraction of *A1*. Stimulus voltage ramp is shown below. *B*: example of a response to a voltage-clamp ramp in the presence of K^+ channel blockers. Raw trace is shown in *B1* and leak subtracted in *B2*. *C*: summary of the effects of channel blockers on the amplitude of PICs. Darker bars represent the peak current of the depolarizing phase of the ramp and light gray bars correspond to the peaks in the hyperpolarizing phase of the ramp. Graphs and error bars are means \pm SE. *D*: current resulting from voltage ramp (black) that was partially blocked by TTX (gray). *E*: example of control currents (black) partially reduced by riluzole (gray). *F*: L-type Ca^{2+} channel blockers, such as nifedipine, also reduce the persistent inward current.

firing lamina I cells predicts the activation of the Ca^{2+} current to be dependent on the persistent Na^+ current and that the maintenance of the Na^+ current will depend on the Ca^{2+} current activation (Prescott and De Koninck 2005). Here both TTX and Cd^{2+} individually are capable of eliminating most of the PICs, suggesting that these currents are largely interdependent to generate PICs.

After spinal transection, a high-threshold current with a delayed activation emerges in a subset of cells. It is possible that this current is required for the spontaneous plateaus seen since they are expressed in the same percentage of cells (28 and 27%, respectively). This current is similar to dendritic L-type calcium currents reported in other regions (Carlin et al. 2000; Mermelstein et al. 2000) and has threshold properties consist-

ent with L-type Ca^{2+} channels (Huang 1989). Self-sustained depolarizations at the offset of current steps and increased firing frequencies during the hyperpolarizing phase of ramps are properties characteristic of cells which generate plateaus. Despite the increased incidence of plateaus and PICs in cells from spinal cord transects, none of these cells displayed self-sustained depolarizations or increased firing frequencies. It is possible that the PICs would become larger at longer durations after spinal cord transection (Li and Bennett 2003). Because the activation of these currents is slow, it is possible that their activation is too delayed to affect spiking during a current ramp. Additionally, the long somatic current steps may not have been depolarizing enough to activate these currents out in the dendrites, possibly explaining the lack of self-sustained depolarization.

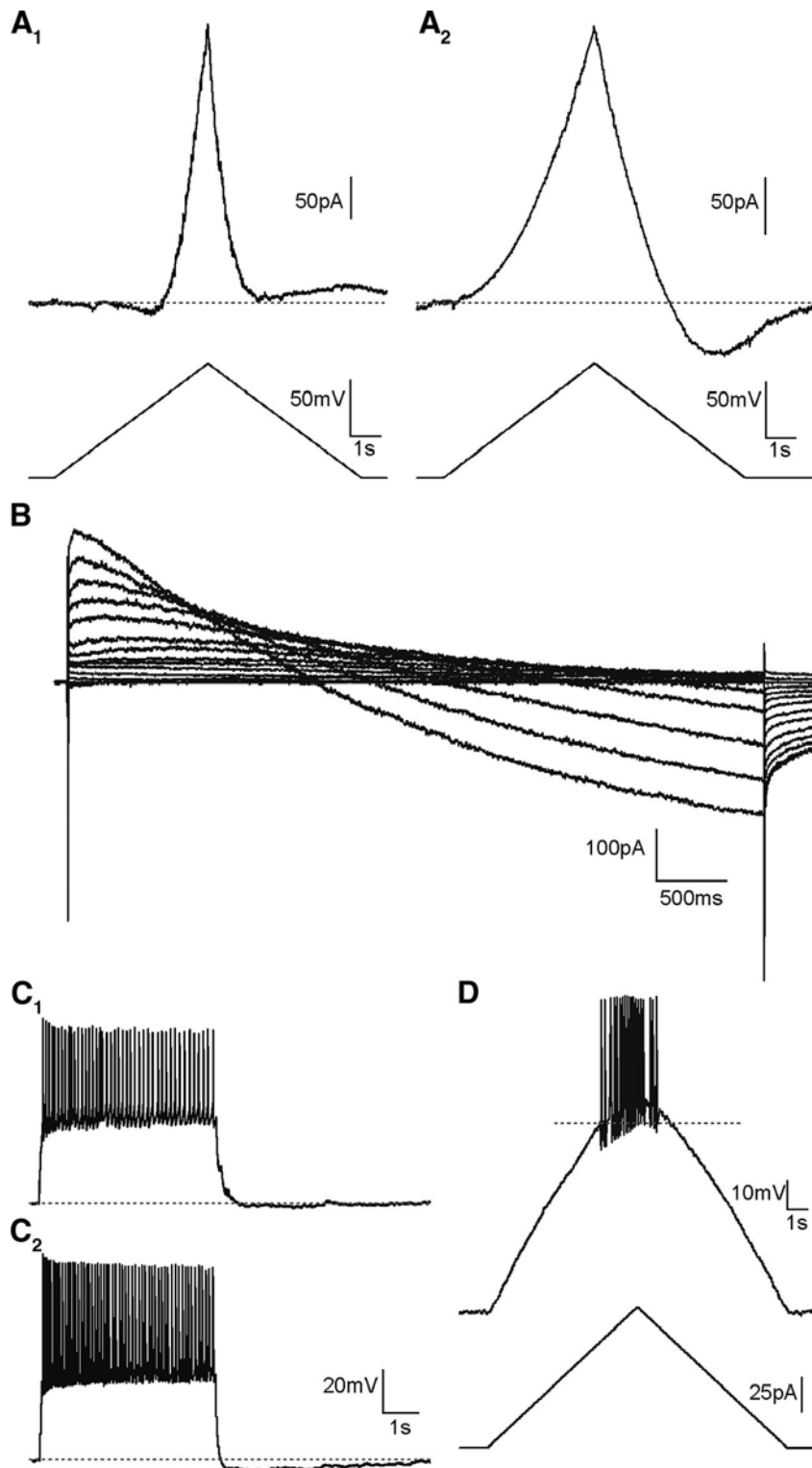


FIG. 8. A high-threshold current with slow activation is seen in some cells from SCI mice. *A*: examples of the responses of 2 cells from SCI mice to a voltage ramp. Both traces have been leak subtracted. Note the lack of PIC in the hyperpolarizing phase in *A1* and the presence of a late activating PIC during the hyperpolarizing phase in *A2*. *B*: current response to 10-mV voltages steps from a holding potential of -80 mV. The slow activating current is seen at high thresholds. *C*: cells from SCI mice did not display self-sustained depolarizations in response to 5-s-long current steps. The cells were brought to approximately -80 mV prior to a 50-pA step. Cells either returned to baseline (*C1*) or hyperpolarized (*C2*) at the end of a step. *D*: response of a cell from a SCI mouse to a current-clamp ramp. Gray dashed line indicates the voltage threshold, which was -43 mV in this cell.

Conclusion

In a subset of lamina I GABAergic neurons, spinal transection induces a more depolarized resting potential and increased firing frequencies and plateau potentials, supporting a resultant increase in neuronal excitability. The mechanisms responsible for altering excitability remain unknown. Because descending modulatory actions are predominantly inhibitory to dorsal horn (Millan 2002) and their actions are lost after chronic cord

transection (see Hadjiconstantinou et al. 1984), an increased GABAergic neuronal excitability may result as part of a compensatory homeostatic response, albeit insufficient.

ACKNOWLEDGMENTS

We thank M. Sawchuk for expert technical assistance. Present address for K. J. Dougherty: Dept. of Neuroscience, Karolinska Institute, 17177 Stockholm, Sweden.

GRANTS

This work was supported by National Institute of Neurological Disorders and Stroke Grant NS-45248 to S. Hochman and Research Service Award NS-49784 to K. J. Dougherty and by Christopher and Dana Reeve Foundation funding to S. Hochman.

REFERENCES

- Anelli R, Sanelli L, Bennett DJ, Heckman CJ.** Expression of L-type calcium channel $\alpha(1)$ -1.2 and $\alpha(1)$ -1.3 subunits on rat sacral motoneurons following chronic spinal cord injury. *Neuroscience* 145: 751–763, 2007.
- Baba H, Ji RR, Kohno T, Moore KA, Ataka T, Wakai A, Okamoto M, Woolf CJ.** Removal of GABAergic inhibition facilitates polysynaptic A fiber-mediated excitatory transmission to the superficial spinal dorsal horn. *Mol Cell Neurosci* 24: 818–830, 2003.
- Bennett DJ, Gorassini M, Fouad K, Sanelli L, Han Y, Cheng J.** Spasticity in rats with sacral spinal cord injury. *J Neurotrauma* 16: 69–84, 1999.
- Bennett DJ, Sanelli L, Cooke CL, Harvey PJ, Gorassini MA.** Spastic long-lasting reflexes in the awake rat after sacral spinal cord injury. *J Neurophysiol* 91: 2247–2258, 2004.
- Bice TN, Beal JA.** Quantitative and neurogenic analysis of the total population and subpopulations of neurons defined by axon projection in the superficial dorsal horn of the rat lumbar spinal cord. *J Comp Neurol* 388: 550–564, 1997.
- Burchiel KJ, Hsu FP.** Pain and spasticity after spinal cord injury: mechanisms and treatment. *Spine* 26: S146–S160, 2001.
- Carlin KP, Jones KE, Jiang Z, Jordan LM, Brownstone RM.** Dendritic L-type calcium currents in mouse spinal motoneurons: implications for bistability. *Eur J Neurosci* 12: 1635–1646, 2000.
- Chen M, Gu JG.** A P2X receptor-mediated nociceptive afferent pathway to lamina I of the spinal cord. *Mol Pain* 1: 4, 2005.
- Chen W, Zhang JJ, Hu GY, Wu CP.** Different mechanisms underlying the repolarization of narrow and wide action potentials in pyramidal cells and interneurons of cat motor cortex. *Neuroscience* 73: 57–68, 1996.
- Chery N, Yu XH, De Koninck Y.** Visualization of lamina I of the dorsal horn in live adult rat spinal cord slices. *J Neurosci Methods* 96: 133–142, 2000.
- Coull JA, Boudreau D, Bachand K, Prescott SA, Nault F, Sik A, De Koninck P, De Koninck Y.** Trans-synaptic shift in anion gradient in spinal lamina I neurons as a mechanism of neuropathic pain. *Nature* 424: 938–942, 2003.
- Craig AD.** The functional anatomy of lamina I and its role in post-stroke central pain. *Prog Brain Res* 129: 137–151, 2000.
- Craig AD.** How do you feel? Interoception: the sense of the physiological condition of the body. *Nat Rev Neurosci* 3: 655–666, 2002.
- Derjean D, Bertrand S, Le Masson G, Landry M, Morisset V, Nagy F.** Dynamic balance of metabotropic inputs causes dorsal horn neurons to switch functional states. *Nat Neurosci* 6: 274–281, 2003.
- Dougherty KJ, Hochman S.** Lamina I GABAergic interneurons become more excitable following spinal cord injury. *Soc Neurosci Abstr* 171.14, 2005.
- Dougherty KJ, Hochman S.** Selective plasticity in a subpopulation of mouse lamina I GABAergic neurons after chronic spinal injury. *Soc Neurosci Abstr* 555.7, 2006.
- Dougherty KJ, Sawchuk MA, Hochman S.** Properties of mouse spinal lamina I GABAergic interneurons. *J Neurophysiol* 94: 3221–3227, 2005.
- Drew GM, Siddall PJ, Duggan AW.** Responses of spinal neurones to cutaneous and dorsal root stimuli in rats with mechanical allodynia after contusive spinal cord injury. *Brain Res* 893: 59–69, 2001.
- Drew GM, Siddall PJ, Duggan AW.** Mechanical allodynia following contusion injury of the rat spinal cord is associated with loss of GABAergic inhibition in the dorsal horn. *Pain* 109: 379–388, 2004.
- Finnerup NB, Jensen TS.** Spinal cord injury pain—mechanisms and treatment. *Eur J Neurol* 11: 73–82, 2004.
- Garraway SM, Mendell LM.** Spinal cord transection enhances afferent-evoked inhibition in lamina II neurons and abolishes BDNF-induced facilitation of their sensory input. *J Neurotrauma* 24: 379–390, 2007.
- Gebhart GF.** Descending modulation of pain. *Neurosci Biobehav Rev* 27: 729–737, 2004.
- Guertin PA.** Semiquantitative assessment of hindlimb movement recovery without intervention in adult paraplegic mice. *Spinal Cord* 43: 162–166, 2005.
- Hadjiconstantinou M, Panula P, Lackovic Z, Neff NH.** Spinal cord serotonin: a biochemical and immunohistochemical study following transection. *Brain Res* 322: 245–254, 1984.
- Hains BC, Klein JP, Saab CY, Craner MJ, Black JA, Waxman SG.** Upregulation of sodium channel Nav1.3 and functional involvement in neuronal hyperexcitability associated with central neuropathic pain after spinal cord injury. *J Neurosci* 23: 8881–8892, 2003a.
- Hains BC, Willis WD, Hulsebosch CE.** Temporal plasticity of dorsal horn somatosensory neurons after acute and chronic spinal cord hemisection in rat. *Brain Res* 970: 238–241, 2003b.
- Hao JX, Kupers RC, Xu XJ.** Response characteristics of spinal cord dorsal horn neurons in chronic allodynic rats after spinal cord injury. *J Neurophysiol* 92: 1391–1399, 2004.
- Hao JX, Xu XJ, Yu YX, Seiger A, Wiesenfeld-Hallin Z.** Baclofen reverses the hypersensitivity of dorsal horn wide dynamic range neurons to mechanical stimulation after transient spinal cord ischemia; implications for a tonic GABAergic inhibitory control of myelinated fiber input. *J Neurophysiol* 68: 392–396, 1992.
- Harvey PJ, Li X, Li Y, Bennett DJ.** 5HT₂ receptor activation facilitates a persistent sodium current and repetitive firing in spinal motoneurons of rats with and without chronic spinal cord injury. *J Neurophysiol* 96: 1158–1170, 2006.
- Heckman CJ, Lee RH, Brownstone RM.** Hyperexcitable dendrites in motoneurons and their neuromodulatory control during motor behavior. *Trends Neurosci* 26: 688–695, 2003.
- Heinke B, Balzer E, Sandkuhler J.** Pre- and postsynaptic contributions of voltage-dependent Ca^{2+} channels to nociceptive transmission in rat spinal lamina I neurons. *Eur J Neurosci* 19: 103–111, 2004a.
- Heinke B, Ruscheweyh R, Forsthuber L, Wunderbaldinger G, Sandkuhler J.** Physiological, neurochemical and morphological properties of a subgroup of GABAergic spinal lamina II neurones identified by expression of green fluorescent protein in mice. *J Physiol* 560: 249–266, 2004b.
- Herrero JF, Laird JM, Lopez-Garcia JA.** Wind-up of spinal cord neurones and pain sensation: much ado about something? *Prog Neurobiol* 61: 169–203, 2000.
- Houngaard J, Kiehn O.** Ca^{++} dependent bistability induced by serotonin in spinal motoneurons. *Exp Brain Res* 57: 422–425, 1985.
- Houngaard J, Kiehn O.** Serotonin-induced bistability of turtle motoneurons caused by a nifedipine-sensitive calcium plateau potential. *J Physiol* 414: 265–282, 1989.
- Houngaard J, Kiehn O.** Calcium spikes and calcium plateaux evoked by differential polarization in dendrites of turtle motoneurons in vitro. *J Physiol* 468: 245–259, 1993.
- Huang LY.** Calcium channels in isolated rat dorsal horn neurones, including labelled spinothalamic and trigeminothalamic cells. *J Physiol* 411: 161–177, 1989.
- Kang J, Huguenard JR, Prince DA.** Voltage-gated potassium channels activated during action potentials in layer V neocortical pyramidal neurons. *J Neurophysiol* 83: 70–80, 2000.
- Kuo JJ, Lee RH, Zhang L, Heckman CJ.** Essential role of the persistent sodium current in spike initiation during slowly rising inputs in mouse spinal neurones. *J Physiol* 547: 819–834, 2006.
- Kuo JJ, Siddique T, Fu R, Heckman CJ.** Increased persistent Na^{+} current and its effect on excitability in motoneurons cultured from mutant SOD1 mice. *J Physiol* 563: 843–854, 2005.
- Li Y, Bennett DJ.** Persistent sodium and calcium currents cause plateau potentials in motoneurons of chronic spinal rats. *J Neurophysiol* 90: 857–869, 2003.
- Malan TP, Mata HP, Porreca F.** Spinal GABA(A) and GABA(B) receptor pharmacology in a rat model of neuropathic pain. *Anesthesiology* 96: 1161–1167, 2002.
- McCormick KA, Srinivasan J, White K, Scheuer T, Catterall WA.** The extracellular domain of the beta 1 subunit is both necessary and sufficient for beta 1-like modulation of sodium channel gating. *J Biol Chem* 274: 32638–32646, 1999.
- Meadows LS, Chen YH, Powell AJ, Clare JJ, Ragsdale DS.** Functional modulation of human brain Nav1.3 sodium channels, expressed in mammalian cells, by auxiliary beta 1, beta 2 and beta 3 subunits. *Neuroscience* 114: 745–753, 2002.
- Melnick IV, Santos SF, Szokol K, Szucs P, Safronov BV.** Ionic basis of tonic firing in spinal substantia gelatinosa neurons of rat. *J Neurophysiol* 91: 646–655, 2004.
- Mermelstein PG, Bito H, Deisseroth K, Tsien RW.** Critical dependence of cAMP response element-binding protein phosphorylation on L-type calcium channels supports a selective response to EPSPs in preference to action potentials. *J Neurosci* 20: 266–273, 2000.

- Millan MJ.** The induction of pain: an integrative review. *Prog Neurobiol* 57: 1–164, 1999.
- Millan MJ.** Descending control of pain. *Prog Neurobiol* 66: 355–474, 2002.
- Monteiro C, Lima D, Galhardo V.** Switching-on and -off of bistable spontaneous discharges in rat spinal deep dorsal horn neurons. *Neurosci Lett* 398: 258–263, 2006.
- Moore KA, Kohno T, Karchewski LA, Scholz J, Baba H, Woolf CJ.** Partial peripheral nerve injury promotes a selective loss of GABAergic inhibition in the superficial dorsal horn of the spinal cord. *J Neurosci* 22: 6724–6731, 2002.
- Morisset V, Nagy F.** Ionic basis for plateau potentials in deep dorsal horn neurons of the rat spinal cord. *J Neurosci* 19: 7309–7316, 1999.
- Murase K, Ryu PD, Randic M.** Substance P augments a persistent slow inward calcium-sensitive current in voltage-clamped spinal dorsal horn neurons of the rat. *Brain Res* 365: 369–376, 1986.
- Pitcher GM, Henry JL.** Cellular mechanisms of hyperalgesia and spontaneous pain in a spinalized rat model of peripheral neuropathy: changes in myelinated afferent inputs implicated. *Eur J Neurosci* 12: 2006–2020, 2000.
- Polgar E, Hughes DI, Riddell JS, Maxwell DJ, Puskar Z, Todd AJ.** Selective loss of spinal GABAergic or glycinergic neurons is not necessary for development of thermal hyperalgesia in the chronic constriction injury model of neuropathic pain. *Pain* 104: 229–239, 2003.
- Prescott SA, De Koninck Y.** Four cell types with distinctive membrane properties and morphologies in lamina I of the spinal dorsal horn of the adult rat. *J Physiol* 539: 817–836, 2002.
- Prescott SA, De Koninck Y.** Integration time in a subset of spinal lamina I neurons is lengthened by sodium and calcium currents acting synergistically to prolong subthreshold depolarization. *J Neurosci* 25: 4743–4754, 2005.
- Ruscheweyh R, Sandkuhler J.** Lamina-specific membrane and discharge properties of rat spinal dorsal horn neurons in vitro. *J Physiol* 541: 231–244, 2002.
- Russo RE, Hounsgaard J.** Plateau-generating neurones in the dorsal horn in an in vitro preparation of the turtle spinal cord. *J Physiol* 493: 39–54, 1996.
- Russo RE, Nagy F, Hounsgaard J.** Modulation of plateau properties in dorsal horn neurons in a slice preparation of the turtle spinal cord. *J Physiol* 499: 459–474, 1997.
- Russo RE, Nagy F, Hounsgaard J.** Inhibitory control of plateau properties in dorsal horn neurons in the turtle spinal cord in vitro. *J Physiol* 506: 795–808, 1998.
- Schoffnegger D, Heinke B, Sommer C, Sandkuhler J.** Physiological properties of spinal lamina II GABAergic neurons in mice following peripheral nerve injury. *J Physiol* 577: 869–878, 2006.
- Stelzner DJ, Weber ED, Prendergast J.** A comparison of the effect of mid-thoracic spinal hemisection in the neonatal or weanling rat on the distribution and density of dorsal root axons in the lumbosacral spinal cord of the adult. *Brain Res* 172: 407–426, 1979.
- Stelzner DJ, Ershler WB, Weber ED.** Effects of spinal transection in neonatal and weanling rats: survival of function. *Exp Neurol* 46: 156–177, 1975.
- Stiller CO, Cui JG, O'Connor WT, Brodin E, Meyerson BA, Linderorth B.** Release of gamma-aminobutyric acid in the dorsal horn and suppression of tactile allodynia by spinal cord stimulation in mononeuropathic rats. *Neurosurgery* 39: 367–374, 1996.
- Suzuki R, Rygh LJ, Dickenson AH.** Bad news from the brain: descending 5-HT pathways that control spinal pain processing. *Trends Pharmacol Sci* 25: 613–617, 2004.
- Theiss RD, Kuo JJ, Heckman CJ.** Persistent inward currents in rat ventral horn neurons. *J Physiol* 580: 507–522, 2007.
- Tillakaratne NJ, de Leon RD, Hoang TX, Roy RR, Edgerton VR, Tobin AJ.** Use-dependent modulation of inhibitory capacity in the feline lumbar spinal cord. *J Neurosci* 22: 3130–3143, 2002.
- Tillakaratne NJ, Mouria M, Ziv NB, Roy RR, Edgerton VR, Tobin AJ.** Increased expression of glutamate decarboxylase (GAD(67)) in feline lumbar spinal cord after complete thoracic spinal cord transection. *J Neurosci Res* 60: 219–230, 2000.
- Todd AJ, Spike RC.** The localization of classical transmitters and neuropeptides within neurons in laminae I–III of the mammalian spinal dorsal horn. *Prog Neurobiol* 41: 609–645, 1993.
- Wiesenfeld-Hallin Z, Aldskogius H, Grant G, Hao JX, Hokfelt T, Xu XJ.** Central inhibitory dysfunctions: mechanisms and clinical implications. *Behav Brain Sci* 20: 420–425, 1997.
- Yoshimura M, Jessell TM.** Primary afferent-evoked synaptic responses and slow potential generation in rat substantia gelatinosa neurons in vitro. *J Neurophysiol* 62: 96–108, 1989.
- Zeilhofer HU.** The glycinergic control of spinal pain processing. *Cell Mol Life Sci* 62: 2027–2035, 2005.
- Zhang H, Xie W, Xie Y.** Spinal cord injury triggers sensitization of wide dynamic range dorsal horn neurons in segments rostral to the injury. *Brain Res* 1055: 103–110, 2005.